Environmental Science & Technology

Article

pubs.acs.org/est

Climate Change and Emissions Impacts on Atmospheric PAH Transport to the Arctic

Carey L. Friedman,*[,†] Yanxu Zhang,[‡] and Noelle E. Selin[§]

[†]Center for Global Change Science, Massachusetts Institute of Technology, Cambridge, Massachusetts 02139, United States

[‡]School of Engineering and Applied Sciences, Harvard University, Cambridge, Massachusetts 02138, United States

[§]Engineering Systems Division and Department of Earth, Atmospheric, and Planetary Science, Massachusetts Institute of Technology, Cambridge, Massachusetts 02139, United States

Supporting Information

ABSTRACT: We investigate effects of 2000−2050 emissions and climate changes on the atmospheric transport of three polycyclic aromatic hydrocarbons (PAHs): phenanthrene (PHE), pyrene (PYR), and benzo[a]pyrene (BaP). We use the GEOS-Chem model coupled to meteorology from a general circulation model and focus on impacts to northern hemisphere midlatitudes and the Arctic. We project declines in anthropogenic emissions (up to 20%) and concentrations (up to 37%), with particle-bound PAHs declining more, and greater declines in midlatitudes versus the Arctic. Climate change causes relatively minor increases in midlatitude concentrations for the more volatile PHE and PYR (up to 4%) and decreases (3%) for particle-bound BaP. In the Arctic, all PAHs decline slightly under future climate (up to 2%). Overall, we observe a small 2050 "climate penalty" for volatile PAHs and "climate benefit" for particle-bound PAHs. The degree of penalty or benefit depends on competition between deposition and surface-to-air fluxes of previously deposited PAHs. Particles and temperature have greater impacts on future transport than oxidants, with particle changes alone accounting for 15% of BaP decline under 2050 emissions. Higher temperatures drive increasing surface-to-air fluxes that cause PHE and PYR climate penalties. Simulations suggest ratios of more-to-less volatile species can be used to diagnose signals of climate versus emissions and that these signals are best observed in the Arctic.

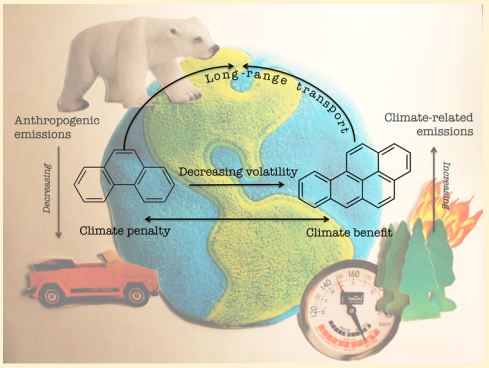

INTRODUCTION

Polycyclic aromatic hydrocarbons (PAHs), toxic compounds produced by the incomplete combustion of organic material, can travel long distances in the atmosphere. As such, PAHs are included in the Convention for Long-Range Transboundary Air Pollution's (CLRTAP's) Persistent Organic Pollutants (POP) protocol.[1] Recently, PAHs have been classified as "emerging contaminants in the Arctic" because body burdens in lower Arctic marine trophic levels are increasing while those of other POPs are declining.[2] Atmospheric transport is the most efficient way for PAHs released in the lower latitudes to reach the Arctic, and previous studies suggest long-range transport accounts for the majority of PAHs observed in Arctic air, especially in winter.[3−7] As conditions in the Arctic become favorable for activities causing local PAH emissions (e.g., transit and/or oil/gas shipping and related accidents/spills, wildfires, domestic combustion),[8−10] and climate changes could lead to alterations in transport and revolatilization,[11−13] it is important to examine the changing influence of long-range transport contributions to Arctic PAH levels. Documenting changes in atmospheric PAH concentrations can provide information to help further analyses of PAH exposure attribute Arctic burdens to specific sources.

PAHs are different from many other POPs in that they are byproducts of combustion (i.e., they are not intentionally produced) and their emissions are ongoing. Emissions of most POPs have been extensively controlled in past decades; thus, most previous studies investigating impacts of future conditions on POP transport have looked primarily at climate changes and not at anthropogenic activities affecting emissions. Lamon et al.[11] examined the multimedia behavior of PCBs under future climate and found increased PCB volatilization and atmospheric transport driven mostly by rising temperatures. Ma and Cao[12] developed an air-surface perturbation model to examine climate change effects on PCBs and pesticides, also finding higher temperatures increase air concentrations. Ma et al.[13] compared Arctic concentrations with simulations of the effect of climate change, finding that a wide range of POPs have already been remobilized in the Arctic because of sea-ice retreat and warming temperatures. Gouin et al.[14] review these and other studies and conclude that climate change will affect POP exposures within a factor of 2. Wöhrnschimmel et al.[15]

Received: March 22, 2013
Revised: November 25, 2013
Accepted: November 26, 2013
Published: November 26, 2013

examined the effects of changing climate and emissions patterns on the distribution of hypothetical POP-like chemicals in the Arctic, finding increases of varying degrees depending on whether emissions were ongoing or phased-out. Collectively, these studies suggest climate change increases air concentrations primarily because higher temperatures induce volatilization from other environmental media. This represents potential for increased transport to remote regions and suggests global efforts to reduce POPs in the environment may be undermined by climate change.[13]

The relative importance of climate versus emissions changes to atmospheric concentrations, however, has not been examined for existing POPs with ongoing emissions. Previous work has investigated the influence of climate versus emissions for atmospheric constituents that simultaneously force climate and degrade air quality, such as ozone (O_3) and particulate matter (PM). Wu et al.[16] examined the influence of 2050 climate and anthropogenic emissions on global O_3, finding that 2050 anthropogenic emissions of O_3 precursors will increase the tropospheric O_3 burden by 17%, while climate-related changes lead to only a 1.6% increase. Pye et al.[17] evaluated the influence of 2050 climate and anthropogenic emissions on inorganic aerosol concentrations, finding considerable increases in global burdens of sulfate, nitrate, and ammonium aerosols under 2050 anthropogenic emissions but either no change or decreases in burdens under 2050 climate. Thus, it has generally been found that emissions reductions or increases dominate changes from climate to 2050; however, emissions impacts are highly uncertain, given the range of assumptions about growth and abatement measures.[18]

Here, we evaluate 2000−2050 changes driven by future climate ("FC") and future emissions ("FE") separately, and together ("FCFE"), on atmospheric PAHs using the chemical transport model GEOS-Chem, with emphasis on transport to the Arctic and concentration changes. We compare emissions, concentrations, deposition, and oxidation globally, in the northern hemisphere (NH) midlatitudes, and in the Arctic to a control simulation of present-day climate and emissions. We also evaluate the impact on PAHs of increased Arctic Ocean oil/gas exploration and transit shipping by including emissions estimates from future shipping in the FCFE scenario. Finally, we explore measurement constraints necessary for resolving anthropogenic versus climate influences on atmospheric PAH observations. Simulations are conducted for phenanthrene (PHE), pyrene (PYR), and benzo[a]pyrene (BaP) to capture a range of volatilities (PHE exists primarily in the gas phase, BaP is mostly particle-bound, and PYR partitions between both phases). We show that while climate change can induce both increases and decreases in atmospheric concentrations, depending on PAH volatility, these changes are minor compared to declines expected from lower anthropogenic emissions.

METHODS

Model Description. We use the chemical transport model GEOS-Chem[19] (http://www.geos-chem.org/) to (1) simulate global atmospheric PAH transport in both the present and future (version 8-03-02) and (2) generate present and future concentrations of species interacting with PAHs (i.e., organic carbon (OC), black carbon (BC), O_3, and hydroxyl radical (OH)) with a NO_x-Ox-hydrocarbon-aerosol simulation (version 9-01-02). Given substantially lower atmospheric PAH concentrations compared to aerosols and oxidants, and the computational intensity of the NO_x-Ox-hydrocarbon-aerosol simulation, we assume PAHs have a negligible impact on aerosols and oxidants and run the PAH and NO_x-Ox-hydrocarbon-aerosol models separately, with monthly mean aerosol/oxidant concentrations archived and used as input to PAH simulations. Sensitivity simulations suggest using daily rather than monthly oxidant and aerosol averages cause ≤2% differences in PAH concentrations (Figure S1; Table S1 in the Supporting Information (SI)). Though there is evidence secondary organic aerosol (SOA) affects atmospheric PAH transport[20] and that it accounts for a substantial (>30%) fraction of total organic matter,[21] analyses of SOA influence on PAH transport suggest it has minimal impact because of the more dominant role of BC versus organic matter in partitioning.[22] The PAH simulation development and evaluation was recently detailed in full elsewhere,[5] and we describe additional updates and re-evaluation in the SI. We use a global primary emissions inventory from 2004 compiled on a country-by-country basis for present-day,[23] with emissions spatially allocated according to population (except for wildfires; see below) on a $1° \times 1°$ grid. The projection of future emissions and meteorology used for both present and future simulations are described below and in the SI. The NO_x-Ox-hydrocarbon-aerosol simulation has also been described extensively elsewhere,[19,24] and we provide a summary of the conditions used here in the SI.

PAH Model Updates. The current model features updates relative to the previous version,[5] which included gas-phase oxidation by OH (scaled for diurnal variation), gas-particle partitioning with OC and BC following the Dachs and Eisenreich scheme,[25] and wet and dry deposition of gases and particles, with equilibrium assumed at each time step. Updates include incorporation of temperature-dependent gas-particle partitioning into the standard simulation, particle-phase PAH oxidation by O_3, and interannual variability in OC, BC, O_3, and OH with concentrations specific to each climate/emissions scenario. Additionally, particles with which PAHs are associated convert from hydrophobic to hydrophilic species with a lifetime of 1.2 days, following a scheme implemented for OC and BC aerosols within GEOS-Chem.[24] This conversion increases the efficiency of wet scavenging over time, with no change in PAH chemistry.

We include two improvements to PAH emissions. First, we alter the primary inventory by redistributing wildfire emissions within the source regions described below, following burned area spatial distribution in the Global Fire Emissions Database (GFED3; http://www.globalfiredata.org). Second, we incorporate re-emissions (i.e., gas-phase diffusive volatilization of previously deposited PAHs) by introducing a level-III fugacity model[26−28] of soil-air and vegetation-air exchange. Re-emissions are sensitive to changes in temperature and atmospheric concentrations. Oceanic re-emissions are not considered as there is no clear indication of PAH outgassing,[29−31] nor from snow/ice surfaces due to lack of data. Though there is evidence of seasonal fluxes from lakes and coastal waters,[32−34] we do not account for them, as the meteorology does not distinguish between solid land surfaces and freshwater. Based on limited data,[32−34] this likely neglects only small fluxes of volatile PAHs in late summer/early fall. Long-range PAH transport is more likely impeded by net absorption by lakes, which also likely has a minimal effect given that surface area and sorption capacity of lakes is small compared to soils, especially those rich in OC.

Meteorology. All simulations are driven by output from the NASA Goddard Institute for Space Studies (GISS) general circulation model (GCM), resolved at 3 or 6 h temporally, 4° latitude × 5° longitude, and 23 levels vertically. For present-day (representing 2000), we use the mean of 1997−2003; for the future (representing 2050), we use the mean of 2047−2053 generated under an SRES A1B scenario; these ranges are sufficient for capturing differences in climate.[17,35]

Methodology Detail in the SI. PAH model details are reported in the SI, including evaluations of model concentration and deposition results against those from its previous publication[5] and observations (Figures S2−S4), development of the re-emissions model, comparisons of simulated re-emissions fluxes and fugacity gradients to observations (Table S2), and physicochemical constants (Table S3). In general, the updated model captures observed monthly mean concentrations and variation with similar or better skill compared to previously published results,[5] while deposition biases high in both versions. Mean PHE, PYR, and BaP observed concentrations are simulated within factors of 1.6, 1.2, and 2.0 (midlatitudes) and 1.1, 1.5, and 2.4 (Arctic), respectively. Summer Arctic simulated concentrations can be orders of magnitude lower than observed, likely due to local sources not considered within the model.[36] Deposition rates are simulated within factors of 2.4, 2.6, and 3.4. Though observations are limited, the re-emissions model predicts net surface-to-air fluxes mostly within the range of observations and captures reported seasonal variations of fugacity ratios (largest ratios in June followed by September and November).

Future Anthropogenic PAH Emissions (FE Scenario). We scale present-day emissions to 2050 for five source regions having potential impacts on the Arctic. Four of the regions are those designated by the Task Force on Hemispheric Transport of Air Pollution (TF HTAP; http://www.htap.org): (Europe: 10W−50E, 25N−65N; North America: 125W−60W, 15N−55N; East Asia: 95 × 10^{-160}E, 15N−50N; South Asia: 50 × 10^{-95}E, 5N−35N). We also scale emissions from Russia (50 × 10^{-180}E, 50N−75N) given their influence on European Arctic concentrations.[3,5]

For each source region, we scale PHE, PYR, and BaP emissions from activities contributing substantially to global Σ16PAH emissions according to projected variables related to each activity. These activities include biomass burning, coke production, domestic coal combustion, and vehicle emissions. We aim to scale present-day emissions to 2050, though in some instances are limited by projections and scale to earlier years as risk-conservative estimates (noted below). For all scaling relying on International Energy Agency (IEA) projections, we use quantities estimated under the IEA's "New Policies Scenario", which assumes cautious global implementation of existing policy commitments.[37] For each PAH, we conduct a ±20% emissions scaling sensitivity analysis, based on uncertainties in the present day inventory, to test the influence of uncertainty in future anthropogenic emissions on results.

Biomass Burning. Traditional biomass burning (the intentional burning of straw, firewood, and animal dung − not including wildfires) is a major source of energy in developing countries but occurs to a lesser degree in developed countries, primarily in wood-burning stoves.[38−40] We scale biomass-burning emissions in East and South Asia according to the IEA's projections for biomass demand in developing countries. As incomes rise, demand is expected to decrease by 60% in China and ∼6% in India between 2008 and 2035.[41] As conservative estimates for 2050, we scale emissions from the entire East and South Asian source regions by these factors, respectively. For all other regions, we do not expect biomass use to change substantially and do not scale emissions.

Coke Production. Global energy consumption in the iron and steel production sector from coking coal use is expected to double between 2000 and 2020 (from ∼300 to 600 million tones of coal equivalent) and then decline until reaching ∼180% of 2000 activity by 2035.[37] Due to lack of regional projections, we scale all source regions by 180% as risk-conservative estimates. Changes in emissions factors (EFs) may play a bigger role in future emissions than increase in coke demand, however. The present-day inventory assumes two types of coke ovens: beehive and large-scale.[42] Beehive ovens have a higher PAH EF than large-scale (490 versus 8 mg/kg, respectively), and the present-day inventory assumes percentage of coke produced by beehive ovens is 15% in China, 5% in India, 1% in Russia, and 0.1% in the U.S. and Europe.[23] These percentages will likely decrease substantially by 2050 in developing countries. Based on discussions elsewhere,[42,43] we assume that beehive oven use will decrease by 2050 to 5% in East Asia, 1% in South Asia, 0.5% in Russia, and 0.05% in the U.S. and Europe, and scale emissions accordingly.

Domestic Coal Combustion. Coal is an important source of cooking fuel and heat in developing countries, particularly in China due to rich reserves.[23] We consider domestic coal a traditional fuel source and scale emissions from its consumption as for biomass burning. Coal combustion for power generation is not considered, as it is a minor part of present-day emissions because of much lower EFs.

Vehicle Emissions. Shen et al.[44] applied EF prediction models to project 1971−2030 PAH emissions from vehicles based on gasoline and diesel consumption estimated under the IPCC A1B scenario. Here, we use Shen et al. 2030 estimates as proxies for 2050. These projections likely overestimate 2050 Asian emissions, as both India and China are projected to experience steep emissions declines starting ∼2030. Though remaining source regions are also projected to experience declines through 2030, the rate of decline is considerably slower.

Arctic Shipping. We project emissions from oil/gas exploration ship activity and transit shipping (Figure S5) following Peters et al.,[8] who estimated 2050 emissions of climate-relevant atmospheric species from expanded Arctic Ocean petroleum and shipping. We calculate 2050 BaP emissions from Arctic shipping by multiplying Peters et al. estimates of 2050 oil/gas exploration and transit shipping BC emissions by a ratio of BaP and BC EFs. We use a BaP EF of 3.3 × 10^{-5} kg/tonne residual fuel oil for a crude tanker at sea[45] and a BC EF of 0.36 kg/tonne residual fuel oil.[8] We assume present-day Arctic shipping emissions are zero.

Particles and Oxidants under FE. A summary of the NO_x-Ox-hydrocarbon-aerosol simulation conditions used to generate aerosol and oxidant concentrations under FE is given in the SI, including assumptions regarding changes in emissions (Tables S4 and S5) and changes in surface concentrations (Figures S6−S9 and Table S6). In general, surface-level OC and BC concentrations decrease, while O_3 and OH increase.

Future Climate (FC Scenario). *Meteorology.* GISS general circulation model data generated under the IPCC's A1B scenario is used to drive PAH transport in future climate. Global mean surface air and land temperatures both increase by 1.6 K, and precipitation increases 5%, with the greatest

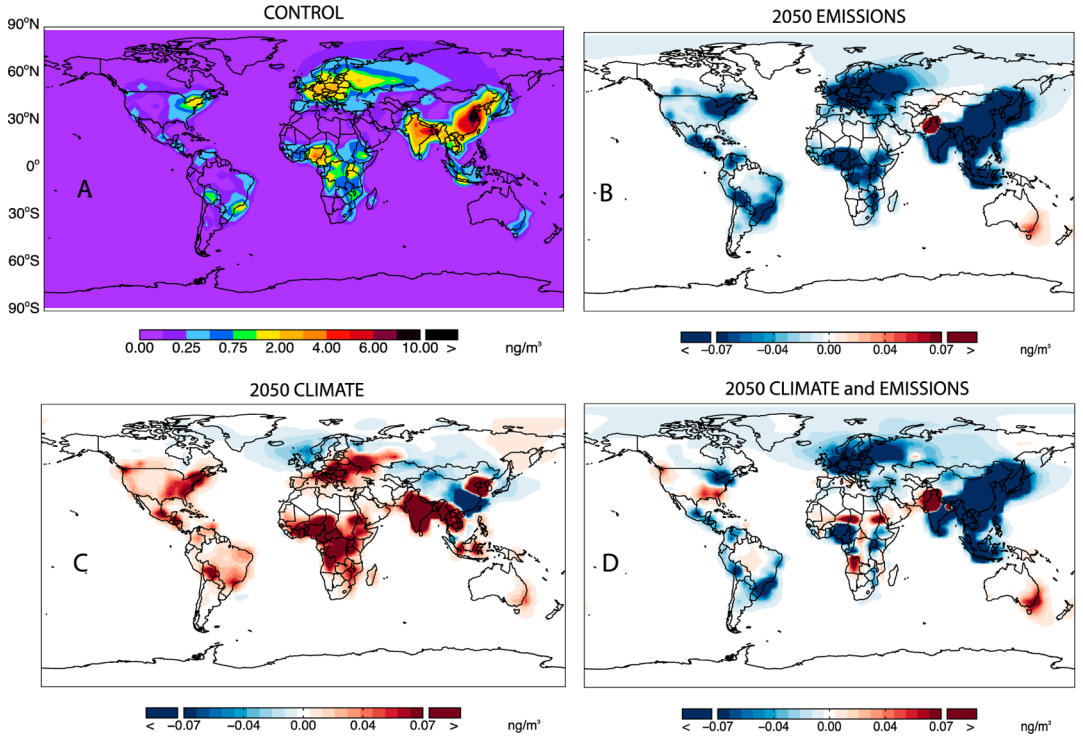

Figure 1. PHE concentrations under (A) the control; concentration differences between the control and simulations under (B) future emissions (FE); (C) future climate (FC); and (D) future climate, future emissions (FCFE). Increases shown in red; decreases in blue.

increases in the intertropical convergence zone. Changes in boundary layer height and less frequent frontal passages cause pollution to linger longer near source regions in the future,[16,17,35] though there is also evidence of a strengthening and northward shift in midlatitude westerlies, particularly in the fall.[17] Further discussion of differences in meteorological variables between future and present-day GCM output can be found elsewhere[16,17,35]

Wildfire Emissions. We scale PAH emissions in the FC scenario to reflect predicted future wildfire activity. The potential for wildfire and length of fire season are expected to increase in many regions from rising temperatures and less precipitation. Though projected changes are uncertain and strongly depend on climate model/emissions scenario, several studies generally agree on wildfire increases in the US, central/southern Europe, and central Asia.[46−49] As upper estimates, we scale emissions from the entire European, North American, and South Asian source regions according to one-half the most extreme increase in fire index predicted under future climate[46]

$$\text{WFI scale factor} = \frac{\text{WFI}_{\text{pres}} + \max(\Delta\text{WFI})/2}{\text{WFI}_{\text{pres}}}$$

where WFI_{pres} is present-day wildfire index and max(ΔWFI) is the maximum difference between future and present-day wildfire index in a given region. There is less agreement on future wildfires in East Asia and Russia. East Asian wildfire potential has been projected to increase but not as greatly as in mid and south Asia.[46−48] Though increases in Siberian fire potential have been projected,[9,50,51] when vegetation is held constant the increase is smaller because of a less flammable resource.[48] This is important because changes in fire potential are expected to occur more rapidly than changes in vegetation.[52] Thus, as risk-conservative estimates, we increase emissions in East Asia by half the increase in South Asia and in Russia by half the greatest predicted increase in annual dangerous fire days.[51] Sensitivities to these assumptions are discussed in the SI.

Particles and Oxidants under FC. A summary of NO_x-Ox-hydrocarbon-aerosol simulation conditions used to generate aerosol and oxidant concentrations under FC, including assumptions regarding changes in natural emissions, is in the SI. In general, the FC simulation produces slightly lower surface-level concentrations of all species compared to the control (Figures S6−S9, Table S6).

RESULTS

Results are presented in the format of the model budget, starting first with PAH sources (emissions), then steady state concentrations, and finally sinks (deposition and oxidation).

Emissions. Each activity's contribution to present-day emissions within each source region is summarized in Tables S7 (anthropogenic) and S8 (climate-related). The contribution of individual activities to present-day emissions varies across regions, though not greatly between PAHs. For example, biomass burning dominates in Asia, while vehicle emissions are most important in North America. Wildfires contribute substantially to present-day emissions in North America and Russia, but matter less in other regions.

Under FE, decreases are observed in all but one region (BaP increases in Russia), with reductions greatest in East Asia and smallest in Russia. Factors for scaling anthropogenic emissions and subsequent changes in totals are presented in Table S7. Conversely, under FC, emissions increase in all regions except East Asia, from as little as 1% in Europe (PYR and BaP) to as much as 16% in North America (PYR).

As with regional, global emissions decrease under FE and increase under FC. Table S9 summarizes global primary, re-,

dx.doi.org/10.1021/es403098w | Environ. Sci. Technol. 2014, 48, 429−437

and total emissions in the control and changes under each future scenario. Under FE, BaP emissions decrease most, and PHE decreases least, while under FC, PHE emissions increase most and BaP least. The discrepancy can be attributed to differences in re-emissions. A substantial fraction (16%) of total PHE emissions are from re-emissions in the control, and this fraction increases (to 19%) under both FE and FC (under FE, because of lower atmospheric concentrations driving greater diffusive net fluxes from surface to air; under FC, because of higher temperatures). These increases offset declining primary emissions under FE and enhance increasing primary emissions under FC. By contrast, only 1% of BaP emissions are from re-emissions in the control, and changes under FC and FE are negligible. Thus, changes in total BaP emissions predominantly reflect primary emissions changes. PYR emissions behave intermediate to PHE and BaP, and emissions in the FCFE scenario are nearly additive combinations of those under FE and FC.

We include projections of BaP emissions from transit and oil/gas exploration shipping in the Arctic in a sensitivity simulation of our FCFE scenario (Figure S5). These emissions total only 1.6 Mg or 0.05% of the global total under FCFE.

Though there is uncertainty in future emissions, predictions generally agree on declines for anthropogenic PAHs and coemitted species.[37,41,44,53] Sensitivity simulations suggest ±20% changes to emissions projections result in, at most, corresponding NH concentration changes of ±11%. Furthermore, a comparison between the relative uncertainties in emissions[23] and the range of physicochemical constants values reported in the literature (Table S10) suggests emissions uncertainties are likely a relatively minor contributor to present-day concentration uncertainties, though this is an area for further research. Thus, we consider projections of PAH emissions relative to one another to be robust.

Concentrations. Figures 1, S10, and S11 (panel A) show the global distributions of PHE, PYR, and BaP total atmospheric concentrations (gas + particulate) in the control, respectively. Panels B, C, and D show the difference in concentration between the FE, FC, and FCFE simulations and the control, respectively. Table S11 summarizes percent change in mean global, NH, midlatitude (5−60°N), and Arctic (60−90°N) concentrations compared to the control. In the control, PHE has the highest concentrations and BaP the least, with highest concentrations closer to areas with high emissions like China and India.

Under FE, concentrations decrease for each PAH. BaP decreases most and PHE least, similar to emissions, and decreases are greatest in the midlatitudes and least in the Arctic. There is also a shift from particles to the gas phase. The shift is greatest for BaP (gas phase increases 2%) because >50% of its mass is particulate (PYR and PHE have <5% and <1% in the particle phase). The shift is due primarily to fewer particles under FE. An FE sensitivity simulation demonstrates that there is no change in particulate/gas speciation when present-day particle concentrations are used. Declining particle concentrations also drive the decrease in total concentrations for particle-bound PAHs under FE: 15%, 10%, and <1% of the decrease in BaP, PYR, and PHE in the NH can be attributed to lower particle concentrations. Arctic concentrations decline less than midlatitudes under FE. Ratios of Arctic to midlatitude concentrations increase; i.e., PAHs are transported to the Arctic more efficiently. The increase in efficiency is greatest for BaP and least for PHE (+23%, +33%, and +47% for PHE, PYR, and BaP, respectively). Some of this is due to lower particle concentrations. For example, a sensitivity simulation of FE with present-day particle concentrations shows BaP and PYR ratios increase less (+41% and +30%, respectively; PHE is not impacted). Overall, simulations suggest the Arctic responds slowly to midlatitudes emissions reductions.

Under FC, only small changes in concentrations are observed and the direction of change depends on the PAH. PHE and PYR concentrations increase slightly everywhere (up to +5%) except over the Arctic, while BaP concentrations decrease slightly (up to −3%). Similar to FE, all PAHs shift to the gas phase, with BaP again showing the greatest shift (+3% in the gas phase). Gas-phase fractions increase primarily from rising temperatures and decreasing particle concentrations. Under FC, volatile PAHs transport to the Arctic less efficiently, and particle-bound PAHs transport more efficiently (i.e., Arctic to midlatitude concentration ratios change by −6%, −4%, and +2%, for PHE, PYR, and BaP, respectively).

As with emissions, concentrations under FCFE are nearly additive combinations of FE and FC. Thus, concentrations decline for all three PAHs, but PHE and PYR experience small "climate penalties", or offsets, in the decreases from anthropogenic emissions due to increases in emissions associated with climate change. The climate penalty is 19% for PHE in the NH and 10% for PYR. Alternatively, BaP experiences a small "climate benefit", in which declining concentrations from anthropogenic emissions are further decreased because of climate changes. The BaP climate benefit is an additional decline of 5% of the anthropogenic decrease. Particle phase shifts are negligible for PHE, but the gas phase increases 2% and 5% for PYR and BaP, respectively. Including projected Arctic shipping emissions in the FCFE simulation diminishes BaP reductions observed without shipping. Thus, in the Arctic there is also a "future shipping penalty" of 21%, but globally and in the midlatitudes the impact is negligible. Though the magnitude of projected shipping emissions is uncertain due to a paucity of ship engine EF data and uncertainties in BC projections,[8] our analysis suggests even moderate increases in Arctic emissions impact otherwise declining concentrations. Other Arctic emissions sources not accounted for here could have similar effects, such as increasing wildfire activity or domestic burning as the region becomes more populated.[54,55]

Uncertainties in simulated concentrations depend on uncertainties in emissions, PAH physicochemical constants, meteorological variables, and aerosol and oxidant concentrations. Sensitivity simulations conducted in a previous study[5] suggest oxidation rate uncertainties have large impacts on simulated concentrations, but the impact on 2000−2050 differences should be relatively minor. Rather, uncertainties in the temperature dependence of partition coefficients and oxidation rate constants (Table S10) are likely to play larger roles in affecting 2000−2050 differences.

Deposition. Table S12 summarizes annual global deposition in the control and changes in each future simulation. In the control, BaP has the greatest fraction of mass removed via deposition (30%) and PHE the least (9%). The contribution of gas versus particulate and wet versus dry to total deposition varies. Particulate wet and dry deposition and gaseous wet deposition are greatest for BaP and least for PHE. Gaseous dry deposition, however, removes the greatest fraction of PYR, followed by PHE and BaP. This is because PYR and PHE have similarly high gas-phase fractions compared to BaP, but gaseous

dry deposition is dependent on the octanol-air partition coefficient (K_{OA}), and the K_{OA} of PYR is >10× greater than that of PHE (Table S3).

Under FE, deposition decreases compared the control. All forms of PHE and PYR deposition decrease, with total deposition reductions of ∼10%. Though declines in BaP particulate deposition drive a total deposition decrease of 10%, gas-phase BaP deposition increases (25% for dry, 15% for wet) because of the substantial shift to the gas phase.

Under FC, small total deposition increases (up to +3%) for each PAH are driven by increasing gas-phase dry deposition (up to +20%, for BaP), which is in turn again due to shifts from the particle to gas phase. All other forms of PHE and PYR deposition decline. Though gaseous BaP wet deposition also increases, it is only a small fraction of the total.

In the FCFE scenario, total PAH deposition decreases, though not by as much as under FE. Thus, we see a climate penalty in deposition for each PAH (up to 30%, for PYR). All forms of deposition decline for PHE and PYR, but there is a nearly 50% increase in gas-phase BaP dry deposition and a 25% increase in gaseous wet deposition because of the substantial shift to the gas phase. These large increases are outweighed by declines in particulate deposition, however.

Deposition is controlled primarily by the air−water partition coefficient (K_{AW}; for wet) and K_{OA} (for dry). Both of these constants have small uncertainty ranges compared to other physicochemical constants (such as k_{OH} or K_{BC}; Table S10). Thus, present-day deposition estimates are likely more robust than other simulated quantities, such as concentration or oxidation, but 2000−2050 changes in deposition may be relatively more sensitive to uncertainties because of the temperature dependence of K_{AW} and K_{OA}.

Oxidation. Table S13 summarizes annual global oxidation in the control and changes in each future scenario. Oxidation accounts for ∼70−90% of atmospheric PAH removal in the control, with OH more important than O_3.

Under FE, gas-phase oxidation by OH increases for each PAH (up to +7%, for BaP). O_3 oxidation decreases for BaP (−4%), and there are negligible changes for PHE and PYR. Combined, the total oxidized fraction increases for each PAH. Changes in oxidation accelerate the decline of gas-phase PAHs. An FE sensitivity simulation with present-day oxidants demonstrates that oxidation increases account for 8%, 10%, and 19% of the decline in NH BaP, PYR, and PHE concentrations, respectively. Increasing oxidation is the main reason for decreasing deposition under FE.

Under FC, BaP oxidation by OH increases (+2%) and by O_3 decreases (−3%), resulting in a 1% decline in total oxidation. There are only very small decreases in PHE and PYR oxidation (<1%). Oxidation does not strongly impact transfer from particles to gas but does limit increasing concentrations of volatile PAHs. For example, even though mean surface-level OH and PHE oxidation decrease under FC, when present-day OH and O_3 concentrations are used in an FC sensitivity simulation, NH PHE concentrations increase by an additional 2%. Also, Arctic concentrations of PHE increase (+4%) rather than decrease, causing the Arctic to midlatitude ratio to decline less (−2%). This is because regions where OH increases under FC (balanced by decreases elsewhere; Figure S6) are also regions with high PAH emissions (e.g., China and Europe).

Under FCFE, total oxidation increases for each PAH (+2%, +2%, and +3% for PHE, PYR, and BaP); this is driven by the increase in OH oxidation under FE.

Given either (1) very large uncertainties in oxidation rate constants because of difficultly with their empirical determination (e.g., k_{OH} for PYR and BaP are calculated from ionization potentials) or (2) oxidation being a major sink for primarily gas-phase PAHs (e.g., PHE), it is likely oxidation rate constant uncertainty contributes substantially to present-day simulated concentration uncertainty. Changes to oxidation in the future are relatively minor compared to changes in other metrics, however, and associated uncertainties remain the same across scenarios, so 2000−2050 differences in oxidation are likely relatively robust.

Using Simulations To Infer Climate versus Anthropogenic Influences in Measurements. We take advantage of the different behaviors of PHE and BaP to examine whether certain locations or seasons are sensitive to future emissions versus climate. We first look at mean annual change in simulated PHE/BaP under FE and FC in the NH (Figure 2)

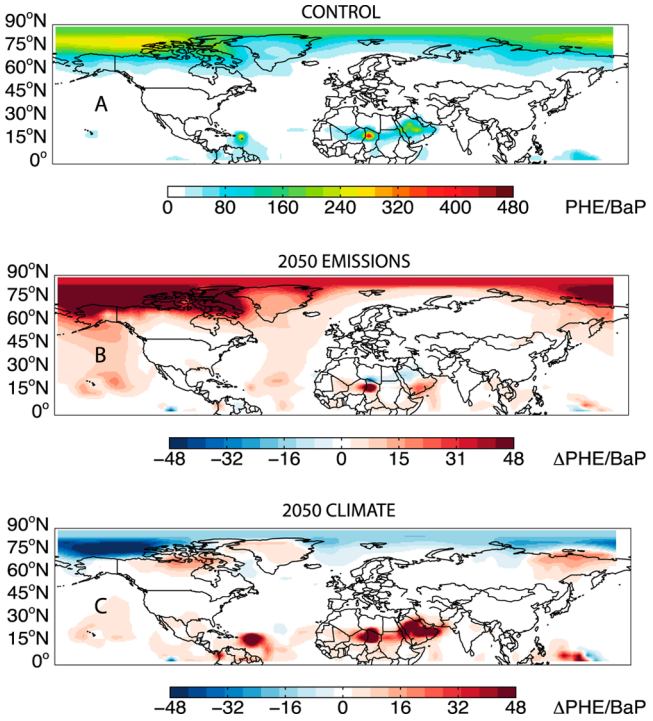

Figure 2. Mean annual northern hemisphere [PHE]/[BaP] in the control (A) and the deviation of this ratio under (B) future emissions (FE), and (C) future climate (FC). Red marks increases; blue marks decreases.

and find that the Arctic, especially northwestern Canada and Alaska, is particularly sensitive to future scenarios, and that the direction of change is opposite for future climate versus emissions. In the control (panel A), the greatest values of PHE/BaP are generally in remote areas, such as in the Arctic, or over areas with low soil organic carbon content and high surface temperatures (e.g., Chad and Niger) which cause large differences in re-emissions. For both FE and FC, the regions where the magnitude of PHE/BaP change is greatest is in similar locations, with FE showing PHE/BaP increases and FC showing declines. We then compare the mean annual simulated PHE/BaP to observed PHE/BaP (Figure S12) over the entire Arctic (60−90N) and in the high Arctic (80−90N). The control simulates the measured ratio from the entire Arctic well, but the relatively small predicted changes from FE and FC are

dx.doi.org/10.1021/es403098w | Environ. Sci. Technol. 2014, 48, 429−437

well within the large standard error of mean observed PHE/BaP. For the high Arctic, however, even though the control biases high compared to observations, predicted changes from FE and FC are greater than the standard error of the observed mean. Comparing observed ratios from the entire Arctic and high Arctic demonstrates that an increasing PHE/BaP value with latitude, as simulated in the control (from 21 to 156), is also detected in observations (from 23 to 80; Figure S12). Neither FE nor FC substantially change PHE/BaP seasonal variation, and no single season clearly resolves the impact of future emissions versus climate.

Uncertainties associated with the FE and FC scenarios need to be considered when interpreting future PHE/BaP, especially under FE given its relatively greater uncertainty. Given differences in PHE and BaP's spatial emissions distributions and nonlinear removal by oxidation, we examine how the FE PHE/BaP ratio is affected when factors for scaling emissions are augmented by ±20% for both PHE and BaP. Though high Arctic concentrations only change by ±8% (PHE) and ±10% (BaP), the FE ratio can range from −17% to +20% or from slightly less than the control ratio to 1.4× the control (Figure S12). The range in the ratio is much smaller when the augmentation is in the same direction for both PAHs; e.g., when both PHE and BaP emissions are reduced by 20%, PHE/BaP changes by only −2%. Thus, the conclusion that PHE/BaP increases under FE is more robust when PHE and BaP emissions decline at similar rates. Observed long-term trends indicate that PHE/BaP in the high Arctic is indeed increasing.[7]

DISCUSSION

2000 to 2050 changes in simulated atmospheric PAH concentrations are driven by declining anthropogenic emissions, with declining concentrations predicted for each PAH simulated. Concentration decreases are more substantial for particle-bound PAHs. This is because PAHs respond differently to climate change depending on their volatility, with behavior under future climate controlled primarily by competition between increasing deposition and increasing re-emissions. Volatile PAH concentrations increase in response to climate change because re-emissions increases outweigh deposition increases, while the opposite is true for particle-bound PAHs. Thus, we observe small "climate penalties" for volatile PAHs (PHE and PYR) and a small "climate benefit" for particle-bound PAHs (BaP).

As mentioned above, though there are substantial uncertainties in emissions projections, quantitative uncertainty analyses suggest emissions play a relatively minor role in simulated present-day concentration uncertainty compared to physicochemical constants.[56] 2000−2050 deposition and re-emissions changes that drive diverging behaviors under future climate are controlled mostly by particle concentrations and the magnitude and temperature-dependence of partition coefficients. This suggests that physicochemical parameters governing these processes (i.e., K_{OA}, K_{BC}, and enthalpies of phase transfer) will have the greatest impacts on whether climate change enhances or offsets declining concentrations from lower emissions. Though oxidation plays a relatively minor role in 2000−2050 concentration changes, there are substantial uncertainties in oxidation reaction rate constants compared to other physicochemical parameters,[56] suggesting greater uncertainty associated with projections of PAHs that are more susceptible to loss via oxidation (e.g., PHE). Thus, while we have confidence that anthropogenic emissions will decline and that PAHs with different volatilities will behave differently in response to climate, the absolute magnitude of the impact on concentrations is less certain, as is the degree to which volatility-dependent behaviors will diverge.

Changes in the simulated PHE/BaP ratio suggest the high Arctic is a priority area for observations aimed at resolving the influence of changing climate versus anthropogenic activities. The fact that the simulated control PHE/BaP ratio in the high Arctic biases high compared to observations should be considered alongside this finding, however. On the model side, annual Arctic PHE concentrations are systematically overestimated and BaP concentrations are underestimated. Uncertainties in measurements may also play a role. Long sampling times required to accumulate detectable masses in the Arctic can lead to known low biases in volatile PAHs (e.g., PHE), while concentrations of low-volatility PAHs (e.g., BaP) are often below analytical limits of quantification (LOQs) (Hayley Hung, personal communication). A common practice for reporting concentrations below LOQs is to estimate true values with a fraction of the LOQ, and this can lead to high biases in lower-volatility PAHs. These factors, combined with the model's ability to simulate concentrations orders of magnitude below LOQs, help explain some of the difference between the control and observed PHE/BaP. Despite this discrepancy, and analytical and practical obstacles associated with measuring PAHs in the high Arctic, our results emphasize the importance of improving long-term measurements within this region. The continued monitoring of PAHs in particular is in accord with the TF HTAP's recommendation that mitigation strategies focus on POPs coemitted with other combustion byproducts because of potential cobenefits.[57]

There are additional uncertainties in our simulations not yet discussed, including but not limited to the parametrization of gas-particle partitioning (e.g., we do not address SOA here), projections of future oxidants and particles, and the influence of other potentially important oxidants (e.g., NO_3). Another substantial uncertainty is how surface-atmosphere exchange will evolve in future climates. In our model, atmospheric PAHs do not interact with surface water, snow, or ice, and results are likely strongly dependent on surface cover parametrizations. Explicitly including these substances and surface-atmosphere exchange could result in considerable differences in Arctic concentrations and thus in our estimates of Arctic PHE/BaP. Ice and snow cover can be efficient scavengers of atmospheric PAHs,[58] and, as such, reduced ice/snow cover could weaken an important atmospheric removal process. Melting ice opens the possibility for air−water exchange and uptake of PAHs into the ocean,[59] and air−water exchange is in turn influenced by changing concentrations of phytoplankton and oceanic OC.[60] At present, little is known about PAH exchange between the atmosphere and Arctic surface environments. Identifying key processes and rates should be a priority for future research, especially given the recent discovery that PAHs dominate the POP body burden of Arctic marine invertebrates and fish,[2] suggesting a complex relationship between the ocean and atmosphere.

We also note that while we assess climate penalties and benefits with respect to atmospheric concentrations, we do not examine the fate of PAHs within other environmental media. It is possible that an atmospheric climate benefit could simultaneously be a lake or soil climate penalty. In addition, given that the greatest increases due to climate changes are no more than +5% of present day concentrations, it is possible that

further studies employing multimedia or ecosystem models may find no basis for concern regarding potential increases in exposures.

Finally, our results should be interpreted within the context of model evaluation against observations. Nearly all of the changes observed under 2050 scenarios are within the range of model-measurement discrepancies (see Figures S2−S4) as well as the range of uncertainty in PAH measurements.

■ ASSOCIATED CONTENT

Supporting Information

Model evaluations, a description of the re-emissions model, and tables and figures summarizing primary and re-emissions, concentrations (PAH, particles, and oxidants), deposition, oxidation, and Arctic PHE/BaP results. This material is available free of charge via the Internet at http://pubs.acs.org.

■ AUTHOR INFORMATION

Corresponding Author

*E-mail: clf@mit.edu.

Notes

The authors declare no competing financial interest.

■ ACKNOWLEDGMENTS

Funding was provided by NSF Atmospheric Chemistry (#1053658), Arctic Natural Sciences (#1203526), and Dynamics of Coupled Natural and Human Systems (#1313755) Programs, and MIT's Leading Technology and Policy Initiative. We thank Glen Peters and Stig Dalsøren (CICERO) for Arctic shipping emissions data, Xu Yue and Bess Corbitt (Harvard University) for discussions surrounding wildfires and providing soil carbon data, respectively, Colin Pike-Thackray (MIT) for physicochemical constant value ranges, and Eric Leibensperger (SUNY Plattsburgh) and Shiliang Wu (MTU) for assistance with GCM data.

■ REFERENCES

(1) UNECE *Protocol to the 1979 Convention on Long-Range Transboundary Air Pollution on Persistent Organic Pollutants*; United Nations Economic Commission for Europe: Aarhus, DM, 1998.

(2) De Laender, F.; Hammer, J.; Hendriks, A. J.; Soetaert, K.; Janssen, C. R. Combining monitoring data and modeling identifies PAHs as emerging contaminants in the Arctic. *Environ. Sci. Technol.* **2011**, *45*, 9024−9029.

(3) Halsall, C. J.; Barrie, L. A.; Fellin, P.; Muir, D. G. C.; Billeck, B. N.; Lockhart, L.; Rovinsky, F.; Kononov, E.; Pastukhov, B. Spatial and temporal variation of polycyclic aromatic hydrocarbons in the Arctic atmosphere. *Environ. Sci. Technol.* **1997**, *31*, 3593−3599.

(4) Halsall, C. J.; Sweetman, A. J.; Barrie, L. A.; Jones, K. C. Modelling the behaviour of PAHs during atmospheric transport from the UK to the Arctic. *Atmos. Environ.* **2001**, *35*, 255−267.

(5) Friedman, C. L.; Selin, N. E. Long-range atmospheric transport of polycyclic aromatic hydrocarbons: A global 3-D model analysis including evaluation of Arctic sources. *Environ. Sci. Technol.* **2012**, *46*, 9501−9510.

(6) Wang, R.; Tao, S.; Wang, B.; Yang, Y.; Lang, C.; Zhang, Y.; Hu, J.; Ma, J.; Hung, H. Sources and pathways of polycyclic aromatic hydrocarbons transported to Alert, the Candian High Arctic. *Environ. Sci. Technol.* **2010**, *44*, 1017−1022.

(7) Becker, S.; Halsall, C. J.; Tych, W.; Hung, H.; Attewell, S.; Blanchard, P.; Li, H.; Fellin, P.; Stern, G.; Billeck, B.; Friesen, S. Resolving the long-term trends of polycyclic aromatic hydrocarbons in the Canadian Arctic atmosphere. *Environ. Sci. Technol.* **2006**, *40* (10), 3217−3222.

(8) Peters, G. P.; Nilssen, T. B.; Lindholt, L.; Eide, M. S.; Glomsrød, S.; Eide, L. I.; Fuglestvedt, J. S. Future emissions from shipping and petroleum activities in the Arctic. *Atmos. Chem. Phys.* **2011**, *11*, 5305−5320.

(9) Flannigan, M. D.; Stocks, B.; Turetsky, M.; Wotton, M. Impacts of climate change on fire activity and fire management in the circumboreal forest. *Glob. Change Biol.* **2009**, *15*, 549−560.

(10) WWF *Oil Spill Response Challenges in Arctic Waters*; Oslo, 2007.

(11) Lamon, L.; von Waldow, H.; MacLeod, M.; Scheringer, M.; Marcomini, A.; Hungerbuhler, K. Modeling the global levels and distribution of polychlorinated biphenyls in air under a climate change scenario. *Environ. Sci. Technol.* **2009**, *43*, 5818−5824.

(12) Ma, J.; Cao, Z. Quantifying the perturbations of persistent organic pollutants induced by climate change. *Environ. Sci. Technol.* **2010**, *44*, 8567−8573.

(13) Ma, J.; Hung, H.; Tian, C.; Kallenborn, R. Revolatilization of persistent organic pollutants in the Arctic induced by climate change. *Nat. Clim. Change* **2011**, *1*, 255−260.

(14) Gouin, T.; Armitage, J. M.; Cousins, I. T.; Muir, D. C. G.; Ng, C. A.; Reid, L.; Tao, S. Influence of global climate change on chemical fate and bioaccumulation: The role of multimedia models. *Environ. Toxicol. Chem.* **2013**, *32*, 20−31.

(15) Wöhrnschimmel, H.; MacLeod, M.; Hungerbühler, K. Emissions, fate and transport of persistent organic pollutants to the Arctic in a changing global climate. *Environ. Sci. Technol.* **2013**, *47*, 2323−2330.

(16) Wu, S.; Mickley, L. J.; Jacob, D. J.; Rind, D.; Streets, D. G. Effects of 2000−2050 changes in climate and emissions on global tropospheric ozone and the policy-relevant background surface ozone in the United States. *J. Geophys. Res.* **2008**, *113*, D18312.

(17) Pye, H. O. T.; Liao, H.; Wu, S.; Mickley, L. J.; Jacob, D. J.; Henze, D. K.; Seinfeld, J. H. Effect of changes in climate and emissions on future sulfate-nitrate-ammonium aerosol levels in the United States. *J. Geophys. Res.* **2009**, *114*, D01205.

(18) Fiore, A. M.; Naik, V.; Spracklen, D. F.; Steiner, A.; Cionni, I.; Collins, W. J.; Dalsøren, S.; Eyring, V.; Folberth, G. A.; Ginoux, P.; Horowitx, L. W.; Josse, B.; Lamarque, J.-F.; MacKenzie, I. A.; Nagashima, T.; O'Connor, F. M.; Righi, M.; Rumbold, S. T.; Shindell, D. T.; Skeie, R. B.; Sudo, K.; Szopa, S.; Takemura, T.; Zeng, G. Global air quality and climate. *Chem. Soc. Rev.* **2012**, *41*, 6663−6683.

(19) Bey, I.; Jacob, D. J.; Yantosca, R. M.; Logan, J. A.; Field, B.; Fiore, A. M.; Li, Q.; Liu, H. X.; Mickley, L. J.; Schultz, M. Global modeling of tropospheric chemistry with assimilated meteorology: Model description and evaluation. *J. Geophys. Res.* **2001**, *106*, 23,073−23,096.

(20) Zelenyuk-Imre, A.; Imre, D.; Beranek, J.; Abramson, E. H.; Wilson, J.; Shrivastava, M. Synergy between secondary organic aerosols and long-range transport of polycyclic aromatic hydrocarbons. *Environ. Sci. Technol.* **2012**, *46*, 12459−12466.

(21) Heald, C. L.; Coe, H.; Jimenez, J. L.; Weber, R. J.; Bahreini, R.; Middlebrook, A. M.; Russell, L. M.; Jolleys, M.; Fu, T.-M.; Allan, J. D.; Bower, K. N.; Capes, G.; Crosier, J.; Morgan, W. T.; Robinson, N. H.; Williams, P. I.; Cubison, M. J.; DeCarlo, P. F.; Dunlea, E. J. Exploring the vertical profile of atmospheric organic aerosol: comparing 17 aircraft field campaigns with a global model. *Atmos. Chem. Phys.* **2011**, *11*, 12673−12696.

(22) Friedman, C. L.; Pierce, J. R.; Selin, N. E. Assessing the influence of secondary organic aerosols on long-range atmospheric PAH transport. *Environ. Sci. Technol.* **2013**, Submitted.

(23) Zhang, Y.; Tao, S. Global atmospheric emission inventory of polycyclic aromatic hydrocarbons (PAHs) for 2004. *Atmos. Environ.* **2009**, *43*, 812−819.

(24) Park, R. J.; Jacob, D. J.; Chin, M.; Martin, R. V. Sources of carbonaceous aerosols over the United States and implications for natural visibility. *J. Geophys. Res.* **2003**, *108* (D12), 4355.

(25) Dachs, J.; Eisenreich, S. J. Adsorption onto aerosol soot carbon dominates gas-particle partitioning of polycyclic aromatic hydrocarbons. *Environ. Sci. Technol.* **2000**, *34*, 3690−3697.

(26) Mackay, D.; Paterson, S. Evaluating the multimedia fate of organic chemics: A level III fugacity model. *Environ. Sci. Technol.* **1991**, *25*, 427−436.
(27) Cousins, I. T.; Mackay, D. Strategies for including vegetation compartments in multimedia models. *Chemosphere* **2001**, *44*, 643−654.
(28) Cousins, I. T.; Mackay, D. Transport parameters and mass balance equations for vegetation in Level III fugacity models. Internal report published on the Web site of the Canadian Environmental Modelling Centre, 2000. http://www.trent.ca/envmodel/ (accessed Dec 2, 2013).
(29) Lohmann, R.; Klanova, J.; Pribylova, P.; Liskova, H.; Yonis, S.; Bollinger, K. PAHs on a West-to-East transect across the Tropical Atlantic Ocean. *Environ. Sci. Technol.* **2013**, *47*, 2570−2578.
(30) Nizzetto, L.; Lohmann, R.; Gioia, R.; Jahnke, A.; Temme, C.; Dachs, J.; Herckes, P.; Di Guardo, A.; Jones, K. C. PAHs in air and seawater along a North-South Atlantic transect: Trends, processes and possible sources. *Environ. Sci. Technol.* **2008**, *42*, 1580−1585.
(31) Lohmann, R.; Gioia, R.; Jones, K. C.; Nizzetto, L.; Temme, C.; Xie, Z.; Schulz-Bull, D.; Hand, I.; Morgan, E.; Jantunen, L. Organochlorine pesticides and PAHs in the surface water and atmosphere of the North Atlantic and Arctic Ocean. *Environ. Sci. Technol.* **2009**, *45*, 5633−5639.
(32) Baker, J. E.; Eisenreich, S. J. Concentrations and fluxes of polycyclic aromatic-hydrocarbons and polychlorinated-biphenyls across the air-water-interface of Lake Superior. *Environ. Sci. Technol.* **1990**, *24*, 342−352.
(33) Nelson, E. D.; McConnell, L. L.; Baker, J. E. Diffusive exchange of gaseous polycyclic aromatic hydrocarbons and polychlorinated biphenyls across the air-water interlace of the Chesapeake Bay. *Environ. Sci. Technol.* **1998**, *32*, 912−919.
(34) Bamford, H. A.; Offenberg, J. H.; Larsen, R. K.; Ko, F. C.; Baker, J. E. Diffusive exchange of polycyclic aromatic hydrocarbons across the air-water interface of the Patapsco River, an urbanized subestuary of the Chesapeake Bay. *Environ. Sci. Technol.* **1999**, *33*, 2138−2144.
(35) Wu, S.; Mickley, L. J.; Leibensperger, E. M.; Jacob, D. J.; Rind, D.; Streets, D. G. Effects of 2000−2050 global change on ozone air quality in the United States. *J. Geophys. Res.* **2008**, *113*, D06302.
(36) Sofowote, U. M.; Hung, H.; Rastogi, A. K.; Westgate, J. N.; Su, Y.; Sverko, E.; D'Sa, I.; Roach, P.; Fellin, P.; McCarry, B. E. The gas/particle partitioning of polycyclic aromatic hydrocarbons collected at a sub-Arctic site in Canada. *Atmos. Environ.* **2010**, *44*, 4919−4926.
(37) IEA. International Energy Agency. *World Energy Outlook 2011*; Paris, France, 2011.
(38) Wenborn, M. J.; Coleman, P. J.; Passant, N. R.; Lymberidi, E.; Sully, J.; Weir, R. A. Speciated PAH inventory for the UK, AEA Technology Environment, Oxfordshire, UK, 1999. <http://www.airquality.co.uk/archive/reports/cat08/0512011419_REPFIN_all_nov.pdf> (accessed Dec 2, 2013).
(39) GLC. Great Lakes Commission. Assessment of Benzo(a)pyrene Air Emissions in the Great Lakes Region: A report of the Great Lakes Regional Toxic Air Emissions Inventory Steering Committee. 2007.
(40) EPA, U.S. 1990 Emissions Inventory of Section 112(c)(6) Pollutants: Polycyclic Organic Matter (POM), TCDD, TCDF, PCBs, Hexachlorobenzene, Mercury, and Alkylated Lead: Final Report, U.S. Environmental Protection Agency, Research Triangle Park, NC, 1998. Available from: <http://www.epa.gov/ttn/atw/112c6/final2.pdf> (accessed Dec 2, 2013).
(41) IEA International Energy Agency. *World Energy Outlook 2010*; Paris, France, 2010.
(42) Bond, T. C.; Streets, D. G.; Yarber, K. F.; Nelson, S. M.; Woo, J. H.; Klimont, Z. A technology-based global inventory of black and organic carbon emissions from combustion. *J. Geophys. Res.: Atmos.* **2004**, *109*, (D14).
(43) Zhang, Y. X.; Tao, S. Emission of polycyclic aromatic hydrocarbons (PAHs) from indoor straw burning and emission inventory updating in China. *Ann. N. Y. Acad. Sci.* **2008**, *1140*, 218−227.
(44) Shen, H.; Tao, S.; Wang, R.; Wang, B.; Shen, G.; Li, W.; Su, S.; Huang, Y.; Wang, X.; Liu, W.; Li, B.; Sun, K. Global time trends in PAH emissions from motor vehicles. *Atmos. Environ.* **2011**, *45*, 2067−2073.
(45) Agrawal, H.; Welch, W.; Miller, J. W.; Cocker, D. R. Emissions measurements from a cruide oil tanker at sea. *Environ. Sci. Technol.* **2008**, *42*, 7098−7103.
(46) Liu, Y.; Stanturf, J.; Goodrick, S. Trends in global wildfire potential in a changing climate. *For. Ecol. Manage.* **2010**, *259*, 685−697.
(47) Scholze, M.; Knorr, W.; Arnell, N. W.; Prentice, I. C. A climate-change risk analysis for world ecosystems. *Proc. Natl. Acad. Sci. U. S. A.* **2006**, *103*, 13116−13120.
(48) Krawchuk, M. A.; Moritz, M. A.; Parisien, M.-A.; Van Dorn, J.; Hayhoe, K. Global pyrogeography: The current and future distribution of wildfire. *PLoS One* **2009**, *4*, e5102.
(49) Spracklen, D. V.; Mickley, L. J.; Logan, J. A.; Hudman, R. C.; Yevich, R.; Flannigan, M. D.; Westerling, A. L. Impacts of climate change from 2000 to 2050 on wildfire activity and carbonaceous aerosol concentrations in the western United States. *J. Geophys. Res.* **2009**, *114*, D20301.
(50) Stocks, B. J.; Fosberg, M. A.; Lynham, T. J.; Mearns, L.; Wotton, B. M.; Yang, Q.; Jin, J.-Z.; Lawrence, K.; Hartley, G. R.; Mason, J. A.; McKenney, D. W. Climate change and forest fire potential in Russian and Canadian boreal forests. *Clim. Change* **1998**, *38*, 1−13.
(51) Malevsky-Malevich, S. P.; Molkentin, E. K.; Nadyozhina, E. D.; Shklyarevich, O. B. An assessment of potential change in wildfire activity in the Russian boreal forest zone induced by climate warming during the twenty-first century. *Clim. Change* **2008**, *86*, 463−474.
(52) Neilson, R. P.; Pitelka, L. F.; Solomon, A. M.; Nathan, R.; Midgley, G. F.; Fragoso, J. M. V.; Lischke, H.; Thompson, K. Forecasting regional to global plant migration in response to climate change. *BioScience* **2005**, *55*, 749−759.
(53) Streets, D. G.; Bond, T. C.; Lee, T.; Jang, C. On the future of carbonaceous aerosol emissions. *J. Geophys. Res.* **2004**, *109*, D24212.
(54) Williams, A.; O'Sullivan Darcy, A.; Wilkinson, A. *The future of Arctic enterprise: Long-term outlook and implications*; Smith School of Enterprise and the Environment, University of Oxford: Oxford, UK, 2011.
(55) Hunsinger, E.; Howell, D. *Alaska Population Projections 2010−2035*; Alaska Department of Labor and Workforce Development: Juneau, Alaska, USA, 2012.
(56) Thackray, C. P.; Friedman, C. L.; Selin, N. E. Parametric uncertainty analysis of PAH simulations using the GEOS-Chem atmospheric chemical transport model. *Environ. Sci. Technol.* **2013**, To be submitted.
(57) Gusev, A.; MacLeod, M.; Bartlett, P. Intercontinental transport of persistent organic pollutants: a review of key findings and recommendations of the task force on hemispheric transport of air pollutants and directions for future research. *Atmos. Pollut. Res.* **2012**, *3*, 463−465.
(58) Daly, G. L.; Wania, F. Simulating the influence of snow on the fate of organic compounds. *Environ. Sci. Technol.* **2004**, *38*, 4176−4186.
(59) AMAP *Arctic Pollution*; Oslo, 2009; p 83.
(60) Galbán-Malagón, C.; Berojalbiz, H.; Ojeda, M.-J.; Dachs, J. The oceanic biological pump modulates the atmospheric transport of persistent organic pollutants to the Arctic. *Nat. Commun.* **2012**, *3*, 862.